available at www.sciencedirect.com

ScienceDirect

journal homepage: www.ejconline.com

MiRNA-29a regulates the expression of numerous proteins and reduces the invasiveness and proliferation of human carcinoma cell lines

M.K. Muniyappa, P. Dowling, M. Henry, P. Meleady, P. Doolan, P. Gammell, M. Clynes, N. Barron *

National Institute for Cellular Biotechnology, Dublin City University, Dublin 9, Ireland

ARTICLE INFO

Article history:
Received 25 June 2009
Received in revised form 31 August 2009
Accepted 11 September 2009
Available online 7 October 2009

Keywords:
In vitro invasion
microRNA
Proteomic profiling
Lung cancer
miR-29a

ABSTRACT

In this study we have identified a functional role for *miR-29a* in cancer cell invasion and proliferation. MiRNA expression profiling of human NSCLC cell lines indicated that *miR-29a* levels were reduced in more invasive cell lines. Exogenous overexpression of *miR-29a* in both lung and pancreatic cancer cell lines resulted in a significant reduction in the invasion phenotype, as well as in proliferation. 2D DIGE proteomic profiling of cells transfected with pre-*miR-29a* or anti-*miR-29a* resulted in the identification of over 100 differentially regulated proteins. The fold change of protein expression was generally modest – in the range 1.2–1.7-fold. Only 14 were predicted computationally to have *miR-29a* seed sequences in their 3′ UTR region.

Subsequent studies using siRNA to knock down several candidate proteins from the 2D DIGE experiment identified RAN (a member of the RAS oncogene family) which significantly reduced the invasive capability of a model lung cancer cell line.

We conclude that *miR-29a* has a significant anti-invasive and anti-proliferative effect on lung cancer cells *in vitro* and functions as an anti-oncomir. This function is likely mediated through the post-transcriptional fine tuning of the cellular levels of several proteins, both directly and indirectly, and in particular we provide some evidence that RAN represents one of these.

© 2009 Elsevier Ltd. All rights reserved.

1. Introduction

MicroRNAs have emerged in recent years as key regulators in a broad spectrum of cellular functions – and dysfunctions – as evidenced by the proliferation of reports in the literature relating to their study. A large proportion of these have been in the field of cancer research with several focused on the invasive/metastatic process specifically.[1]

One of the challenges of studying miRNA function in the cellular environment is identifying potential protein targets. Many early studies started with the target gene, often well associated with some aspect of cancer, and then tried to identify miRNAs that might bind the transcript based on *in silico* predictions.[2,3] Conversely, *in silico* analysis has been used to predict the potential target genes based on the sequence of a particular miRNA.[4] The rules being used to develop these algorithms are becoming more refined as experimental data builds, leading to improved predictive capacity of these software tools. More recently, high throughput proteomic and transcriptomic technologies have greatly increased the identification and understanding of bona fide miRNA targets in cell lines, tissue samples and *in vivo*.[5]

* *Corresponding author:* Tel.: +35 317005804; fax: +35 317005484.
E-mail address: niall.barron@dcu.ie (N. Barron).
0959-8049/$ - see front matter © 2009 Elsevier Ltd. All rights reserved.
doi:10.1016/j.ejca.2009.09.014

In this study we were interested in identifying downstream targets of *miR-29a* using such approaches. *MiR-29a* is found on chromosome 7q32.3 in tandem with *miR-29b-1* and has been reported in studies focused on cancer biomarker identification[6] as well as cancer-related phenotypes *in vitro* and *in vivo*. It has been shown to regulate the levels of Mcl-1 and subsequently increase TRAIL-mediated apoptosis in malignant cholangiocarcinoma cells.[3] TCL-1, the oncogene implicated in progression of CLL, has been shown to be regulated, at least in part, by the action of *miR-29a*.[7] In lung cancer cell lines *miR-29a* was shown to reverse aberrant methylation by down-regulating the expression of DNMT3A and 3B.[4] Importantly, a study by Chang and colleagues demonstrated that *miR-29a* is a target for suppression by *c-myc*.[8] Preliminary work in our laboratory identified *miR-29a* as being differentially expressed in an *in vitro* model of invasive lung cancer. In combination these findings point to an important role for this molecule in maintaining normal cellular function and behaviour and prompted us to further investigate other potential target proteins and pathways influenced by *miR-29a* in our model system.

2. Materials and methods

2.1. Cell culture

Lung carcinoma cell lines, DLKP and DLKP-A[9] were maintained in ATCC media supplemented with 5% FCS and incubated at 37 °C. DLKP is a poorly differentiated, squamous cell lung carcinoma with a non-invasive phenotype. DLKP-A is a highly invasive variant generated by chronic exposure of the parent cell line to the chemotherapeutic drug, Adriamycin. PANC-1 cell line is a highly invasive cell line derived from a pancreatic ductal carcinoma (ATCC) and maintained in DMEM supplemented with 5% (v/v) FCS and incubated at 37 °C.

2.2. Transfection of cells

The cells were transfected in suspension after trypsinisation with 50 nM siRNA, anti-miR or pre-miR (Applied Biosystems). For the invasion assay, 3×10^5 cells per millilitre were transfected per well of a 24-well plate. For proliferation, 3×10^4 cells were seeded per well of a 96-w plate. Transfection complexes were prepared in OptiMEM (Invitrogen) with 0.15 μl/96-well or 2 μl/24-well of siPORT NeoFx transfection agent (Ambion). Seventy-two hours post-transfection, the cells were lysed for qRT-PCR analysis or Western blot, and assayed for proliferation or used to seed an *in vitro* invasion assay. For stable plasmid transfections 2 μg DNAs were used to transfect 3×10^5 cells in 2 ml in a 6-well plate. Forty-eight hours post-transfection the medium was supplemented with 800 μg/ml G418 and selection was continued until the mock-transfected cells were killed. Surviving cells were expanded and single-cell cloned by the limiting dilution method.

2.3. Detection of mature miR-29a by qRT-PCR

MiR-29a quantification was performed according to the primer/probe assay protocol provided by the manufacturer (Applied Biosystems). For the RT step, 25 ng RNA was used to generate cDNA. Quantitative PCR was performed by the addition of 2× Taqman Universal Mastermix containing the appropriate probe/primer mix. RNU6B expression was used for internal normalisation. All reactions were performed on an AB7500 instrument and relative expression was calculated using the $2^{-\Delta\Delta Ct}$ method in SDS 1.3 software.

2.4. In vitro proliferation and invasion assay

The cell numbers were assessed 72 h post-transfection using the acid phosphatase method.[10] Invasion assays were performed using Matrigel™ invasion assays (BD Bioscience). After rehydration of the matrix, the medium underneath the insert was replaced with ATCC media containing 5% (v/v) FCS. Seventy-two hours after miRNA/siRNA transfections, the cells were trypsinised, counted and resuspended in media containing 5% (v/v) FCS at a density of 1×10^6 cells/ml. Hundred microlitres of cell suspension was added to each insert. The cells were incubated at 37 °C for 24–48 h, after which the inserts were stained, washed and the number of invasive cells were determined by counting 10 random fields at 20× magnification.

2.5. Detection of mRNA levels of siRNA knockdown gene targets

RNA was isolated from post-siRNA-transfected cells using the RNeasy Mini Prep Kit® (Qiagen) and quantified using a Nanodrop™ spectrophotometer. For each reaction 500 ng RNA was used to generate cDNA using a high-capacity cDNA reverse transcription kit (Applied Biosystems). SybrGreen™-based qRT-PCR analysis was performed with specific primers designed for each target. Primers used were (a) RAN (sense 5′-GTTGGTGATGGTGGTACTGGAA-3′, antisense 5′-TCCTCTGTTGGTGTGGAACACT-3′) and (b) B-actin (sense5′-AGCAGGAGTATGACGAGTCCG-3′, antisense 5′-TCCCAGGGAGACCAAAAGC-3′). Each PCR contained 400 nM of sense and antisense primers and 50 ng of cDNA. There were technical as well as biological triplicates of each sample. Target gene expression levels were normalised using β-actin.

2.6. Plasmid constructs

The *miR-29a* expression vector was constructed by PCR amplification of ~250 bp sequence from DLKP genomic DNA. This contained the complete pre-*miR-29a* sequence and additional sequence upstream and downstream. The primers used were sense 5′-AAACCGGATCCGAGCCCAATGTATGCTGGATTTAG-3′ (BamHI site underlined) and antisense 5′-CCCAACTCGAGTTAAGCTTTGTTTTCTTAGTTCTTGTCCATGG-3′ (HindIII site underlined). PCR amplification was performed with KOD-XL High Fidelity PCR kit (Merck/Novagen), using 0.7 μg template in a 50 μl reaction mixture, according to the manufacturers protocol. Thermal cycler conditions were 95 °C for 2 min, followed by 30 cycles of 94 °C for 30 s, 60 °C for 5 s and 72 °C for 30 s. The PCR product was digested with BamHI/HindIII and ligated into pSilencer™ 4.1-CMV-Neo vector (Ambion).

The RAN 3′ UTR sequence was amplified from DLKP-A-derived total RNA using custom primers: sense 5′-

AAAAAGCTTTGAGAATGAAGCTGGAGCCCAG-3′ (HindIII site underlined) and antisense 5′-CCCGGATCCCGGCTTGCG-TATCAACT TCACA-3′ (BamHI site underlined). The amplified PCR product was digested with HindIII/BamHI and cloned downstream of *gfp* in pEGFP-C1 vector (Clontech).

3. 2D Difference gel electrophoresis (2D DIGE)

DLKP-A cells were transfected with pre-*miR-29a*, anti-*miR-29a* or their negative controls for 72 h and harvested. Lysates were minimally labelled with 200 pmol/50 μg of protein with either Cy3 (control) or Cy5 (test) for comparison on the same gel (dyes from GE Healthcare). A pool containing equal amounts of all samples was also prepared and labelled with Cy2 to be used as an internal standard on all gels to aid image matching and cross-gel statistical analysis. Three biological repeats of each transfected sample were preformed. Twelve gels were generated in total, with two gels per comparison.

Immobilised 24 cm linear pH gradient (IPG) strips (GE Healthcare), pH 3–11, were rehydrated in rehydration buffer (7 M urea, 2 M thiourea, 4% CHAPS, 0.5% IPG Buffer, 50 mM DTT) overnight. 2D DIGE was performed according to the manufactures instructions and as previously described.[11] The gels were scanned with a Typhoon variable mode imager (GE Healthcare) and the subsequent gel images were imported into the BVA module of DeCyder 6.5 software. Proteins were defined as differentially regulated if the observed fold change was ±1.2 ($p < 0.05$) in 1-WAY ANOVA between negative and pre- or anti-*miR-29a*-treated samples.

3.1. Protein identification by mass spectrometry

Protein digestion and MALDI-TOF MS were performed as described previously.[11] For MALDI-TOF MS analysis, protein identification was achieved using the PMF Profound database search engine for peptide mass fingerprints. Low abundance proteins were identified using LC–MS/MS with an Ettan MDLC system (GE Healthcare) in high throughput configuration directly connected to a Finnegan LTQ (Thermo Electron). The peptides were concentrated and desalted on RPC trap columns (Zorbax 300SB C18, 0.3 mm × 5 mm, Agilent Technologies), and were separated on a nano-RPC column (Zorbax 300SB C18, 0.075 mm × 100 mm, Agilent Technologies) using a linear acetonitrile gradient from 0% to 65% over 60 min. All buffers used for nano LC separation contained 0.1% formic acid (Fluka) as the ion-pairing reagent. Full scan mass spectra were recorded in profile mode and tandem mass spectra in centroid mode. The peptides were identified using the information in the tandem mass spectra by searching against the SWISS PROT database using SEQUEST.

3.2. Criteria for protein identification

For protein identification, artificial modifications of peptides (carbamidomethylation of cysteines and partial oxidation of methionines) were considered. Searches were also carried out allowing for one missed cleavage. Protein identifications were accepted if they could be established at greater than 99.8% probability and had at least two identified peptides.

3.3. Western blotting

Western blotting was performed on protein cell lysates (7 M urea, 2 M thiourea, 4% CHAPS, 30 mM Tris/HCl, pH 8.5) with 20 μg/lane of protein separated on a 12% NuPAGE Bis–Tris gel (Invitrogen). After transfer to Hybond-ECL nitrocellulose (GE Healthcare) the membranes were blocked and incubated with rabbit anti-human RAN (Abcam) (1:500) with 5% (w/v) fat-free milk powder in PBS containing 0.5% Tween-20, or mouse anti-human GAPDH (1:3000) overnight at 4 °C. Secondary antibodies were added after washing and bound antibody was detected using enhanced chemiluminescence (ECL).

3.4. Flow cytometer analysis

Stable GFP overexpressing DLKP-A cells were trypsinised from 24-well plates and resuspended at <500 cells/μl. The benchtop cytometer (Guava Technologies) was set up using GFP-negative DKLP-A cells to adjust the flow rate and gate the negative population (green fluorescence <10 with PMT gain at 600 V). GFP-transfected cells were then analysed and the intensity of fluorescence was captured for 5000 cells per sample.

4. Results

4.1. MiR-29a is down-regulated in invasive cancer cells

An initial bioarray-based study in our laboratory comparing microRNA expression in non- and highly invasive variants of the lung cancer cell line DLKP identified several differentially expressed miRNAs, one of which was *miR-29a*. Subsequent measurement by qRT-PCR confirmed that *miR-29a* expression in the invasive variant was less than 45% of that in the non-invasive cell line (Fig. 1).

4.2. MiR-29a decreases the invasive phenotype of cancer cells in vitro

Though ectopic expression of *miR-29a* has previously been shown to reduce the growth of lung cancer cells *in vitro* and their tumourigenic potential *in vivo*,[4] we were interested to see if it would impact on the invasiveness of DLKP-A cells. The cells were transfected with a short, artificial *miR-29a* mimic (pre-miR) and seeded on ECM (Matrigel™) 72 h later in a

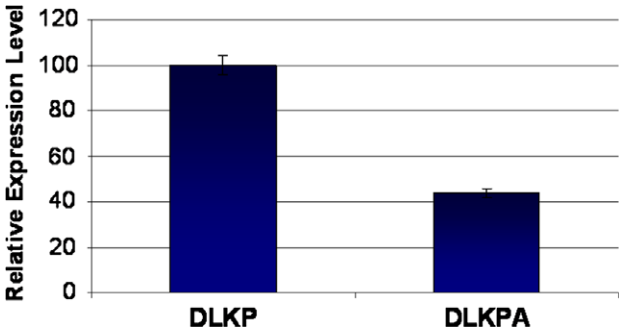

Fig. 1 – Endogenous *miR-29a* expression levels in DLKP compared to DLKP-A. The samples were normalised using RNU6B expression ($n = 3$).

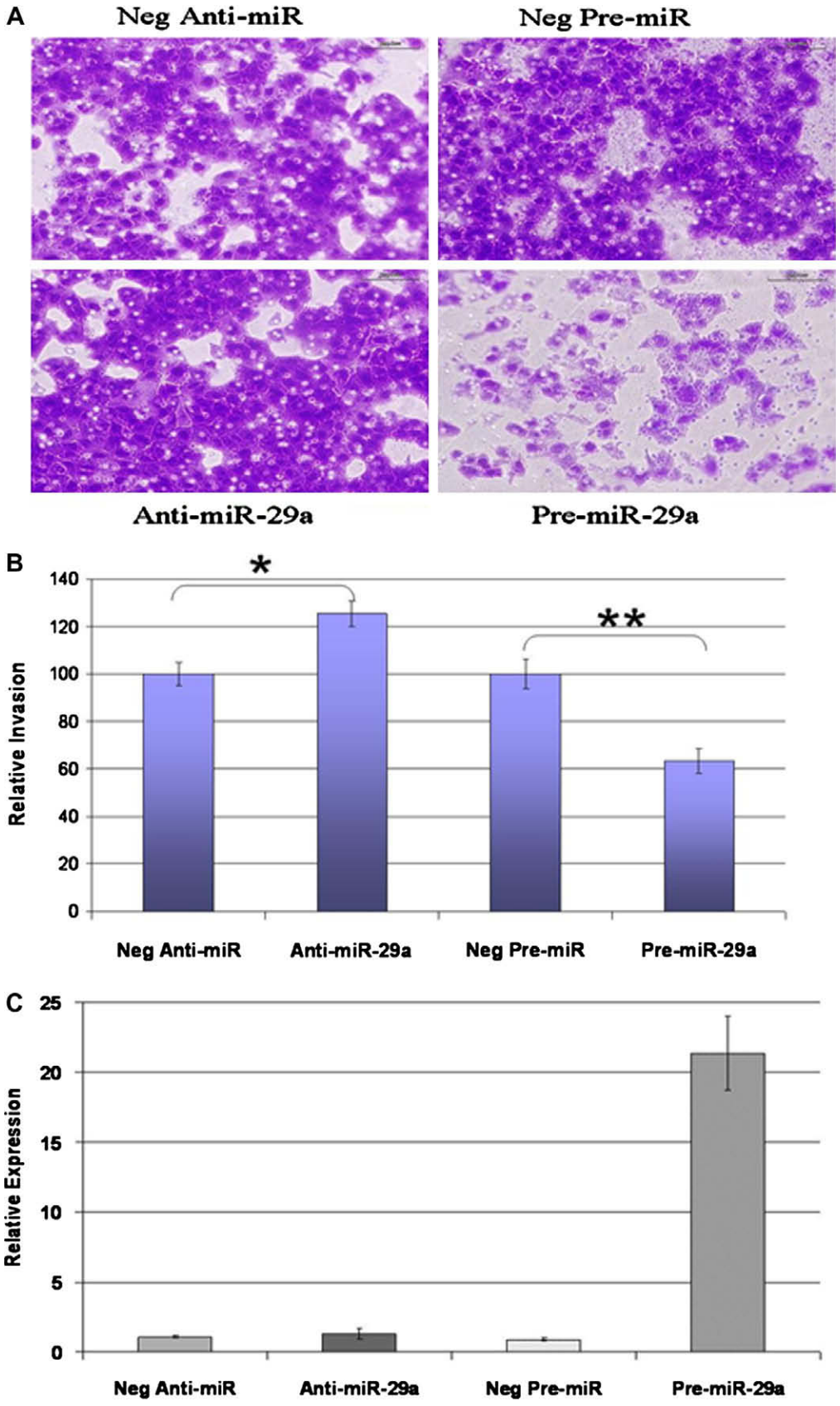

Fig. 2 – Effect of *miR-29a* disregulation on invasion in DLKP-A cells. (A) Representative field of view of *in vitro* invasion inserts at 20× magnification. (B) Quantification of relative numbers of invading cells representing average counts from 10 fields-of-view per 2 inserts per sample ±SD, $^{*}p < 0.0005$, $^{**}p < 10^{-4}$. qRT-PCR to detect relative *miR-29a* levels in control (neg), anti- and pre-*miR-29a*-transfected cells (C).

Boyden chamber *in vitro* invasion assay. Compared to cells transfected with a non-specific pre-miR control sequence, we observed a 35–40% reduction in invading cells 24 h later (Fig. 2a and b). The reciprocal experiment where endogenous *miR-29a* activity was inhibited by transient transfection with a complementary single-stranded RNA molecule (anti-mir) increased the invasiveness of DLKP-A cells compared to the control, though the effect was less pronounced possibly due to the already highly invasive phenotype of these cells. To confirm that the transfections resulted in the desired impact on cellular levels of *miR-29a*, qRT-PCR was performed on extracted total RNA. Though the pre-miR treatment increased the detected *miR-29a* by greater than 20-fold, we were unable to detect any change in target levels subsequent to anti-miR transfection (Fig. 2c). This is most likely due to the fact that these molecules merely act as inhibitors by competitively binding the target (mature *miR-29a*) but do not induce degradation, as in the case of siRNA action.

The impact of exogenous upregulation of *miR-29a* in DLKP-A cells led us to question whether the effect would prove to be tissue-type specific or more general. The highly invasive human pancreatic carcinoma cell line, PANC-1, was transfected with pre-miR and similarly displayed a 50% reduction in its capacity to invade through the matrix (Fig. 3a and b). Quantitative PCR suggested upregulation of *miR-29a* in these cells compared to the negative control (Fig. 3c) though not to the same extent achieved in the DLKP-A cell line.

Further confirmation of its impact on the invasiveness was demonstrated in stable DLKP-A clones that constitutively overexpressed *miR-29a*. These were generated by cloning a ~250 bp genomic fragment from DLKP-derived DNA, that included the full *miR-29a* sequence and flanking sequence, into an expression vector. Stable clones were found to express mature *miR-29a* at varying levels (Fig. 4b). The invasiveness of a sub set of these clones was measured and found to correlate negatively with expression of *miR-29a* (Fig. 4a). It was also found that the proliferation of these stable clones was reduced compared to control cells (Fig. 4c); this was not observed in the transient transfections.

4.3. *Proteomic profiling of cells overexpressing miR-29a*

A small number of gene targets of *miR-29a* activity *in vitro* or *in vivo* have been verified experimentally in several recent publications. These include Tcl1,[7] the DNA methyltransferase enzymes, DNMT3A and B,[4] Mcl-1,[3] ColA1,[12] tristetraprolin[13] and CDC42.[14] In addition, depending on which software algorithm is employed, several hundred more downstream targets can be *in silico* predicted. To gain a better understanding of the range of proteins affected either directly or indirectly by this miRNA *in vitro*, we applied 2D DIGE analysis of lysates from DLKP-A cells transfected transiently with exogenous pre- and anti-*miR-29a* compared to cells treated with the appropriate non-specific, negative controls. As

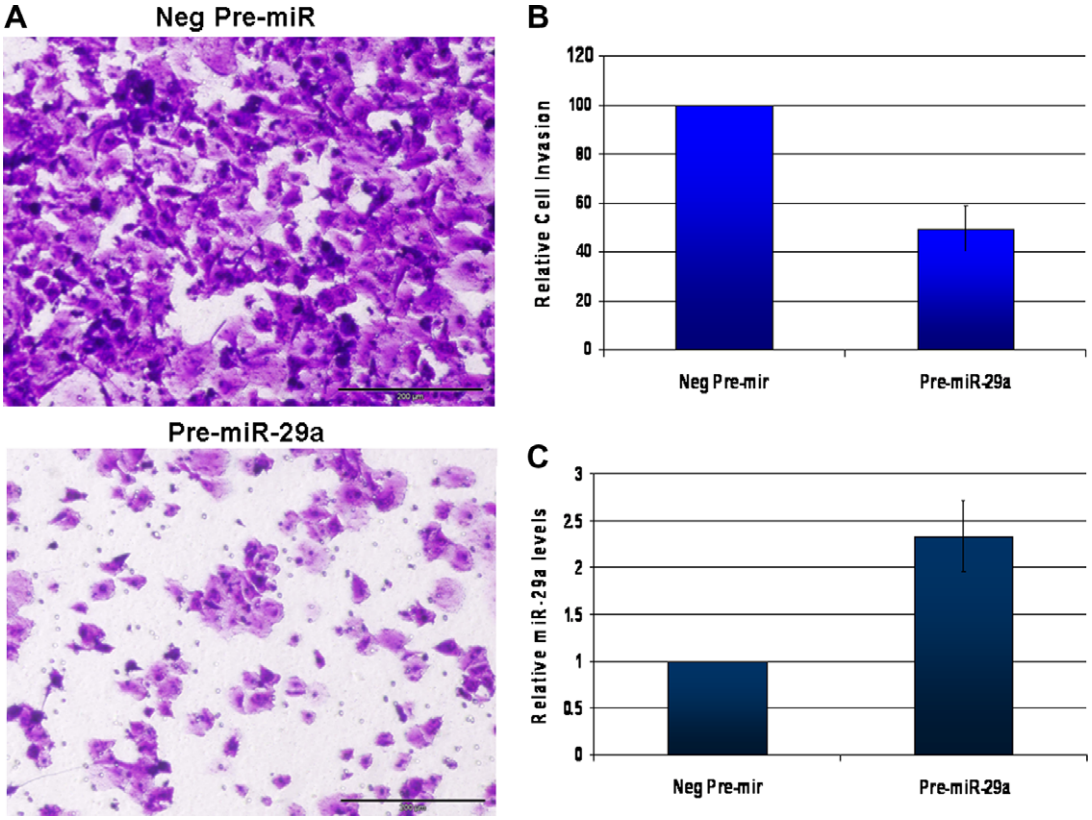

Fig. 3 – Effect of *miR-29a* upregulation on invasion in PANC-1 cells. (A) Representative field of view of *in vitro* invasion inserts under 20× magnification. (B) Quantification of relative numbers of invading cells representing average counts from 10 fields of view in 2 Boyden chambers (error bar represents ±SE, $p < 0.02$). (C) qRT-PCR to detect relative *miR-29a* levels in control and pre-*miR-29a*-transfected cells ($n = 2$, $p = 0.13$, error bars ± SE).

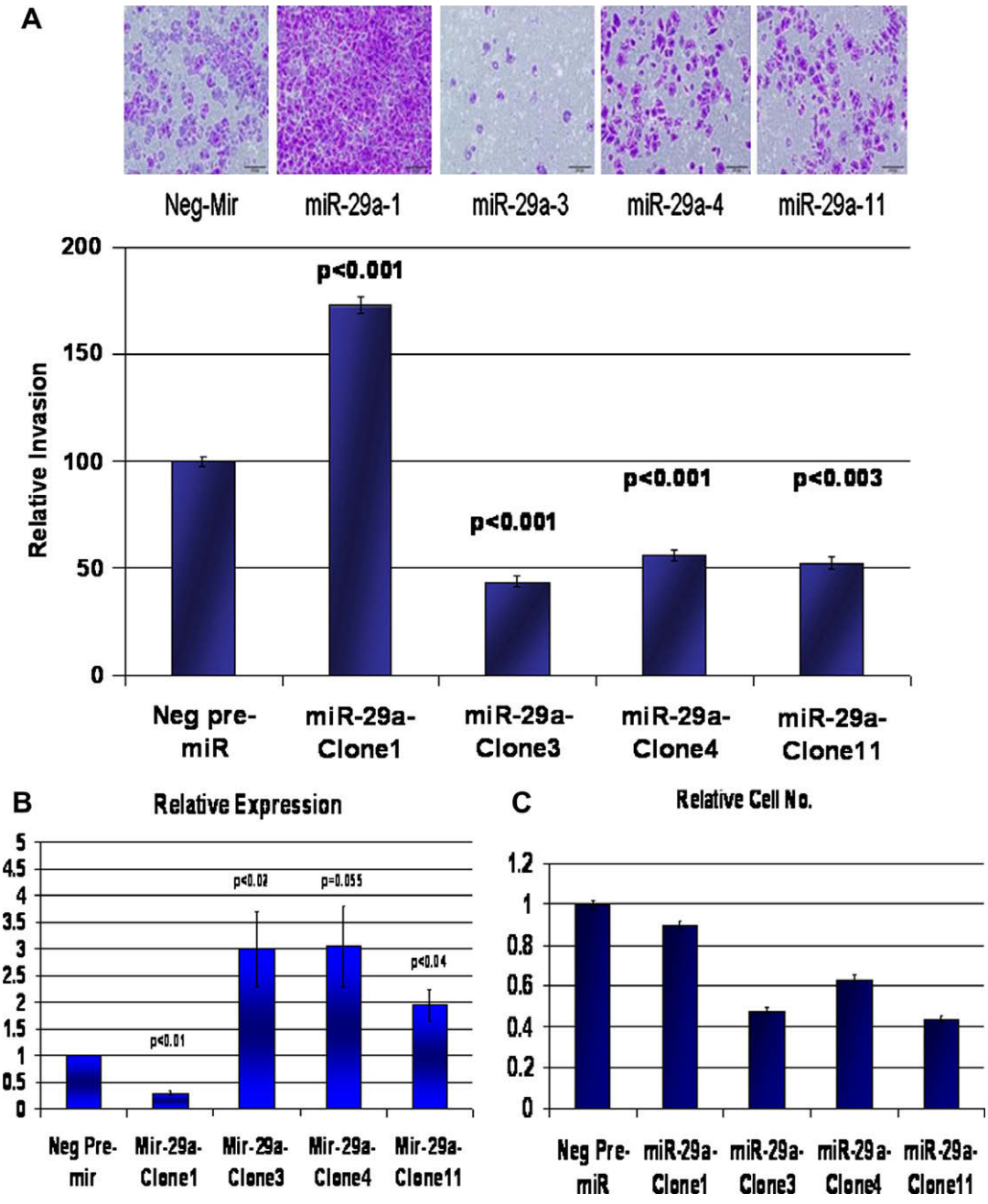

Fig. 4 – Invasive phenotype of DLKP-A clones stably transfected with *miR-29a* or Neg-mir expression vector. (A) Relative invasion of each of the clones compared to a negative-mir clone. Neg-Mir represents a clone derived from cells stably transfected with the expression vector incorporating a non-specific sequence of similar length to the *mir-29a* insert ($n = 3$, error bars ± SE). (B) Relative expression of *miR-29a* in stable clones ($n = 3$, error bars ± SE). (C) Cell proliferation of the 5 clones relative to Neg Pre-mir, ($p < 0.001$ in all samples, error bars ± SE).

expected, the protein spots were observed in both treatments that were both increased and decreased compared to the control-transfected cells. To simplify the subsequent analysis we focused on the proteins that were down-regulated in response to pre-miR treatment and up-regulated in anti-miR-treated cells. These comprised the primary list of 75 potentially 'direct' targets of *miR-29a* activity (Table 1). The proteins with the opposite trend in expression, i.e. up-regulated upon treatment with pre-*miR-29a* or down-regulated upon treatment with anti-*miR-29a*, would be expected to be indirect, downstream targets of *miR-29a* action. However, it is likely that some of the proteins on the primary list could also be indirect targets whose expression is affected by the action of a *miR-29a* target gene. In addition, several proteins were identified at more than one spot location suggesting the presence of post-translational modifications on these molecules.

The range of differential expression of the identified proteins was modest with the greatest change being 1.63-fold down-regulation of macrophage migration inhibitory factor

Table 1 – Proteins differentially regulated after transient transfection of invasive DLKP-A lung cancer cells with Pre- or Anti-miR-29a. The cell lysates were separated by 2D DIGE followed by identification of differential protein spots by either MALDI-TOF or LC–MS. Identifications were only sought for proteins up-regulated in response to anti-*miR-29a* transfection (+'ve FC) or down-regulated subsequent to pre-*miR-29a* transfection (–'ve FC). A fold change cut-off of 1.2 was applied with a *p*-value < 0.05. Prediction of the presence of a *miR-29a* seed region in the 3′ UTR of each gene was performed with RNA hybrid software.

Gene symbol	Gene name	Protein ID	GenBank ID	Mass (Da)	Fold change	ANOVA	Predicted target of *miR-29a*	Biological process
HIST4H4*	Histone H4	gi|75061938|	NM_175054	11,360	–1.64	0.034		Chromatin packaging and remodelling
MIF	Macrophage migration inhibitory factor	gi|1170955|	NM_002415	12,468	–1.63	0.035		Macrophage-mediated immunity
ISG15	ISG15 ubiquitin-like modifier	gi|386837|	NM_005101	17,910	–1.63	0.0026		Proteolysis
PRDX1*	Peroxiredoxin 1	gi|548453|	NM_002574	22,096	–1.53	0.035		Antioxidation and free radical removal
CFL1	Cofilin-1	gi|116848|	NM_005507	18,491	–1.53	0.0019		Apoptosis
PEBP1	Phosphatidylethanolamine-binding protein 1	gi|1352726|	NM_002567	21,044	–1.53	0.0004	x	Other signal transduction
HIST4H4*	Histone H4	gi|75061938|	NM_175054	11,360	–1.46	0.0011		Chromatin packaging and remodelling
LGALS1	Histidine triad nucleotide-binding protein 1	gi|42542978|	NM_002305	14,910	–1.45	0.0005		Cell adhesion; other immune and defence; induction of apoptosis
RPL11	60S ribosomal protein L11	gi|51701767|	NM_000975	20,240	–1.45	0.0005		Protein biosynthesis
RPS12	40S ribosomal protein S12	gi|133742|	NM_001016	14,517	–1.43	0.012		Protein biosynthesis
GMFB	Glia maturation factor beta	gi|46577593|	NM_004124	16,703	–1.43	0.0021	x	Neurogenesis
BTF3L4	Transcription factor BTF3 homologue 4	gi|75042131|	NM_152265	17,260	–1.43	0.0019		Unclassified
CLPP	ATP-dependent Clp protease proteolytic subunit	gi|3023512|	NM_006012	30,161	–1.42	0.03		Proteolysis
FABP5	Fatty acid-binding protein, epidermal	gi|232081|	NM_001444	15,155	–1.42	0.005		Lipid and fatty acid transport
HIBCH	3-Hydroxyisobutyryl-CoA hydrolase	gi|146324905|	NM_014362	43,454	–1.42	0.005		Carbohydrate metabolism and fatty acid beta-oxidation
PPIB	Cyclosporin	gi|1310882|	NM_000942	19,700	–1.41	0.027	x	Protein folding; nuclear transport; immunity and defence
PSMB4	Proteasome subunit beta type-4 precursor	gi|116242733|	NM_002796	29,186	–1.41	0.0024		Proteolysis
PPIA*	Peptidylprolyl isomerase A (cyclophilin A)	gi|75766275|	NM_021130	18,030	–1.4	0.0045	x	Protein folding; nuclear transport; immunity and defence
SOD1	Superoxide dismutase	gi|134611|	NM_000454	15,926	–1.39	0.043		Immunity and defence

Table 1 – (*continued*)

Gene symbol	Gene name	Protein ID	GenBank ID	Mass (Da)	Fold change	ANOVA	Predicted target of *miR-29a*	Biological process
GSTK1	Glutathione S-transferase kappa 1	gi|12643338|	NM_015917	25,480	–1.39	0.0015		Translational regulation
PPIA*	Peptidylprolyl isomerase A (cyclophilin A)	gi|3659980|	NM_021130	18,090	–1.36	0.02	x	Protein folding; nuclear transport; immunity and defence
TPx-B	Thioredoxin Peroxidase B	gi|9955016|	NM_005809	21,680	–1.36	0.0011		Unknown
APRT	Adenine phosphoribosyltransferase	gi|114074|	NM_000485	19,595	–1.35	0.015		Unclassified
PPIA*	Peptidylprolyl isomerase A (cyclophilin A)	gi|75766275|	NM_021130	18,030	–1.35	0.0091	x	Unknown
IGH2bM35a	Immunoglobulin heavy chain	gi|7161037|	AJ253041	10,600	–1.35	0.004		Unknown
RAN	RAS-related nuclear protein	gi|5107684|	NM_006325	23,300	–1.35	0.00024		RNA localisation; intracellular signalling cascade; nuclear transport and cell cycle
ATP6V1E1	Vacuolar ATP synthase subunit E 1	gi|549207|	NM_001696	26,129	–1.34	0.013		Nucleoside, nucleotide and nucleic acid metabolism
PRDX1*	Peroxiredoxin 1	gi|548453|	NM_002574	22,096	–1.34	0.0035		Antioxidation and free radical removal
HINT1	Histidine triad nucleotide-binding protein 1	gi|1708543|	NM_005340	13,793	–1.33	0.0048		Unclassified
GNB2L1	Guanine nucleotide-binding protein subunit beta-2-like 1	gi|54037164|	NM_006098	35,055	–1.32	0.048		Signal transduction; protein targeting
PRDX3	Peroxiredoxin 3 isoform b	gi|32483377|	NM_006793	26,110	–1.32	0.0031		Antioxidation and free radical removal
ARL3*	ADP-ribosylation factor-like protein 3	gi|543851	NM_004311	20,443	–1.31	0.046	x	General vesicle transport
PRDX1*	Peroxiredoxin 1	gi|55959887|	NM_002574	19,130	–1.31	0.019		Antioxidation and free radical removal
PPIA*	Peptidylprolyl isomerase A (cyclophilin A)	gi|2981764|	NM_021130	18,090	–1.31	0.0069	x	Unknown
SFRS1	Splicing factor, arginine/serine-rich 1	gi|45708738|	NM_006924	22,560	–1.29	0.042		mRNA splicing
ERP29	Endoplasmic reticulum protein ERp29 precursor	gi|6015110|	NM_006817	28,975	–1.29	0.0027		Constitutive exocytosis
CMPK1	Cytidine monophosphate kinase	gi|12644008|	NM_016308	22,208	–1.29	0.00039	x	Pyrimidine metabolism
C20orf45	Chromosome 20 open reading frame 45	gi|26392626|	NM_016045	21,481	–1.28	0.019		Unclassified
PSMA2*	Proteasome subunit alpha type-6	gi|46397655|	NM_002791	27,382	–1.28	0.017		Proteolysis
NDKA	Nucleoside diphosphate kinase A	gi|127981|	NM_198175	17,138	–1.28	8.40E–05		Pyrimidine metabolism
VBP1	VHL-binding protein-1	gi|1465751|	NM_003372	19,520	–1.27	0.015		Protein folding and protein complex assembly
HPRT	Hypoxanthine phosphoribosyltransferase	gi|459815|	NM_000194	24,730	–1.27	0.0046		Purine metabolism
THOC6	THO complex subunit 6 homologue	gi|74759455|	NM_024339	37,511	–1.26	0.023		Unclassified

(*continued on next page*)

Table 1 – (*continued*)

Gene symbol	Gene name	Protein ID	GenBank ID	Mass (Da)	Fold change	ANOVA	Predicted target of *miR-29a*	Biological process
PRDX1*	Peroxiredoxin 1	gi|55959887|	NM_002574	19,130	–1.26	0.015		Antioxidation and free radical removal
Sfrs3	Splicing factor, arginine/serine-rich 3	gi|51338673|	NM_003017	19,318	–1.26	0.011		mRNA splicing
CFL1	Cofilin-1	gi|116848|	NM_005507	18,491	–1.26	0.0024		Cell structure
PARK7	Parkinson disease (autosomal recessive, early onset) 7	gi|42543006|	NM_007262	20,060	–1.26	0.00072		Cell proliferation and differentiation
GNB3	Guanine nucleotide-binding protein subunit beta-3	gi|121011|	NM_002075	37,197	–1.25	0.048		G-protein mediated signalling
GRB2	Growth factor receptor-bound protein 2	gi|28876|	NM_002086	18,620	–1.25	0.0059		Receptor protein tyrosine kinase signalling pathway
ESD	Esterase D/ formylglutathione hydrolase	gi|12654663|	NM_001984	32,020	–1.25	0.0013		Unclassified
NDUFA10	NADH dehydrogenase (ubiquinone) 1 alpha subcomplex	gi|13097333|	NM_004544	41,070	–1.25	0.0013		Oxidative phosphorylation
LYPLA2	Lysophospholipase II	gi|41017276|	NM_007260	24,721	–1.25	0.0003		Lipid metabolism; cell proliferation and differentiation
PRDX1*	Peroxiredoxin 1	gi|55959887|	NM_002574	19,130	–1.24	0.037		Antioxidation and free radical removal
FKBP3	FK506-binding protein 3	gi|232096|	NM_002013	25,161	–1.24	0.03		Protein folding and cell cycle control
HSPB1	Heat shock protein beta-1	gi|19855073|	NM_001540	22,769	–1.24	0.03		Protein folding and stress response
CYC	Cytochrome c	gi|42560195|	NM_018947	11,741	–1.24	0.018	x	Oxidative phosphorylation; apoptotic processes
ANXA1	Annexin A1	gi|113944|	NM_000700	38,690	–1.24	0.006		Fatty acid metabolism; receptor-mediated signal transduction and cell motility
PSMA2*	Proteasome subunit alpha type-2	gi|39644890|	NM_002787	24,970	–1.23	0.0096		Proteolysis
PRDX6	Peroxiredoxin-6	gi|1718024|	NM_004905	25,019	–1.22	0.041	x	Antioxidation and free radical removal
PGAM1	Phosphoglycerate Mutase	gi|67464305|	NM_002629	29,970	–1.22	0.0021		Glycolysis
GALE	UDP-galactose-4-epimerase	gi|68056598|	NM_001008216	38,257	–1.21	0.037		Carbohydrate metabolism
PSMB2	Proteasome subunit beta type-2	gi|1709762|	NM_002794	22,822	–1.21	0.029	x	Proteolysis
ANXA2	Annexin A2	gi|56967119|	NM_001002858	36,640	–1.21	0.0059	x	Intracellular protein traffic; Mesoderm development; Cell structure and motility
PAFAH1B2	Platelet-activating factor acetylhydrolase IB subunit beta	gi|55977293|	NM_002572	25,553	–1.21	0.0043		Unclassified

Table 1 – (*continued*)

Gene symbol	Gene name	Protein ID	GenBank ID	Mass (Da)	Fold change	ANOVA	Predicted target of *miR-29a*	Biological process
CACYBP	Calcyclin-binding protein	gi|46576651|	NM_014412	26,194	–1.2	0.036		Proteolysis
HIBADH	3-Hydroxyisobutyrate dehydrogenase	gi|12643395|	NM_152740	35,306	–1.2	0.0074		Amino acid biosynthesis and amino acid catabolism
IGv	Immunoglobulin heavy chain subgroup VIII V-D-J region	gi|348186|		13,830	–1.2	0.0036		Unclassified
KIAA1598	Formin-like (pthr23213:sf23)	gi|156637366|	NM_018330	71596	1.21	0.034		Cell motility
RuvB-like 2	48 kDa TATA box-binding protein-interacting protein	gi|28201890|	NM_006666	51125	1.22	0.049		mRNA transcription regulation; Embryogenesis; Mesoderm development
ACTC1	Alpha-actin-1	gi|55976646|	NM_005159	42024	1.22	0.036	X	Exocytosis; Endocytosis; Transport; Cytokinesis; Cell structure
ATP5A1	ATP synthase subunit alpha, mitochondrial precursor	gi|158514235|	NM_001001937	59714	1.22	0.013		UnClassified
EEF1A1	Eukaryotic translation elongation factor 1 alpha 1	gi|31092|	NM_001402	50450	1.23	0.022		Translational regulation
ENO1	Enolase-alpha	gi|31873302|	NM_001428	47420	1.24	0.055		Glycolysis
PGK1	Phosphoglycerate kinase 1	gi|48145549|	NM_000291	44980	1.24	0.036		Glycolysis
CCT3	T-complex protein 1 subunit gamma	gi|66774185|	NM_005998	60495	1.24	0.024		Protein folding;Protein complex assembly
SERBP1	Plasminogen activator inhibitor 1 RNA-binding protein	gi|52783206|	NM_001018067	44939	1.24	0.0036		UnClassified
EF2	Elongation factor 2	gi|119172|	NM_001961	95277	1.25	0.051		Protein biosynthesis
TRXR1	Thioredoxin reductase 1	gi|50403780|	NM_003330	55490	1.25	0.02		Electron transport;Other metabolism
LOC652797	Pyruvate kinase isozymes M1/M2	gi|20178296|	XM_001719890	57900	1.27	0.024		Unknown
GRP94	Heat shock protein gp96 precursor	gi|15010550|	NM_003299	90350	1.28	0.055		Protein folding;Stress response
ALDH1A1	Aldehyde dehydrogenase 1	gi|2183299|	NM_000689	55440	1.28	0.047		Other carbon metabolism
PTBP1	Polypyrimidine tract-binding protein 1	gi|131528|	NM_002819	57186	1.29	0.0074		mRNA splicing
DDT	D-dopachrome decarboxylase	gi|2828192|	NM_001355	12704	1.35	0.039		Macrophage-mediated immunity

* Indicates proteins that were identified at more than one spot location suggesting isoforms with post-translational modifications

(MIF) upon pre-*miR-29a* treatment but more typically in the range 1.2–1.4-fold. *In silico* analysis of the 3′ UTRs of these genes predicted that only 14 contained potential 'seed' sequences, i.e. at least 6 matches between nt2–8 at the 5′ end of *miR-29a*. Analysis of the proteins on the primary list to investigate the cellular functions that they have been previously associated with revealed a bias towards proliferation, apoptosis, secretion and motility (Table 1).

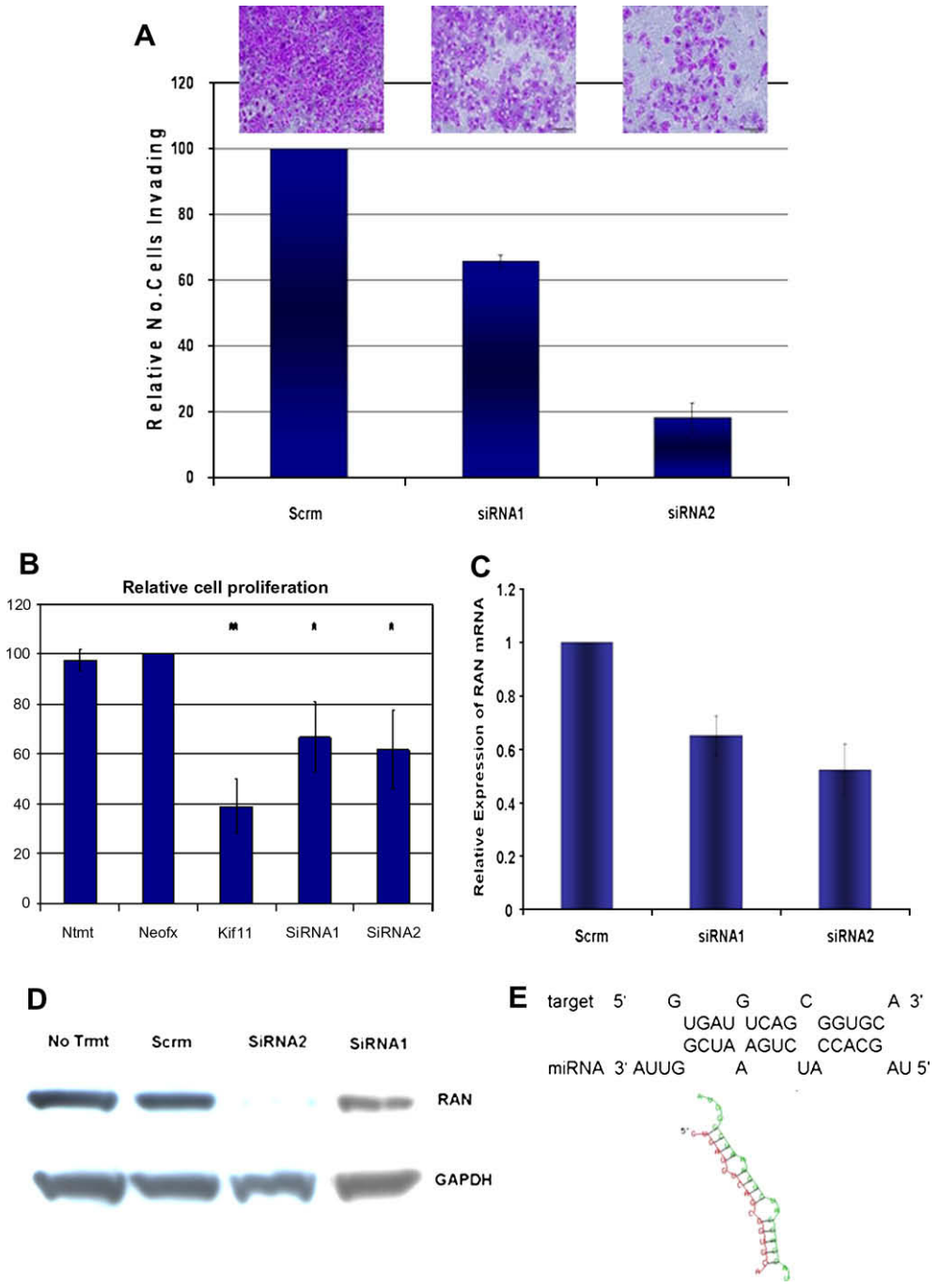

Fig. 5 – Impact of RAN-specific knockdown on DLKP-A cells using 2 independent siRNA sequences. (A) Specific knockdown of RAN by transient transfection of siRNA in DLKP-A reduces *in vitro* invasion (±SD, $p < 10^{-6}$). (B) proliferation, (±SD, $^{*}p < 0.02$, $^{**}p < 0.0001$), Kif11 denotes *kinesin* positive control. Ntmt = no treatment, Scrm = scrambled control siRNA. (C) Confirmation of siRNA-induced knockdown of RAN mRNA by qPCR (±SE, $n = 2$). (D) protein by Western blot. (E) RNA hybrid software-predicted interaction between *miR-29a* and the RAN 3′ UTR.

4.4. *Functional investigation of miR-29 target proteins*

A small panel of the identified proteins was chosen to investigate the impact of knocking down their expression individually *in vitro*. These targets included Annexin A2 (ANXA2), growth factor receptor-bound 2 (GRB2), macrophage migratory inhibitory factor (MIF) – which had the highest fold change after pre-*miR-29a* treatment – and Ras-related nuclear protein (RAN). The latter three were chosen based on previous associations with an invasive phenotype or metastatic disease, whereas ANXA2 was picked based on *in silico* predictions of a *miR-29a* binding site. Though siRNA-mediated knockdown was verified in all cases by qRT-PCR (data not shown), only RAN depletion impacted on the invasiveness of DLKP-A

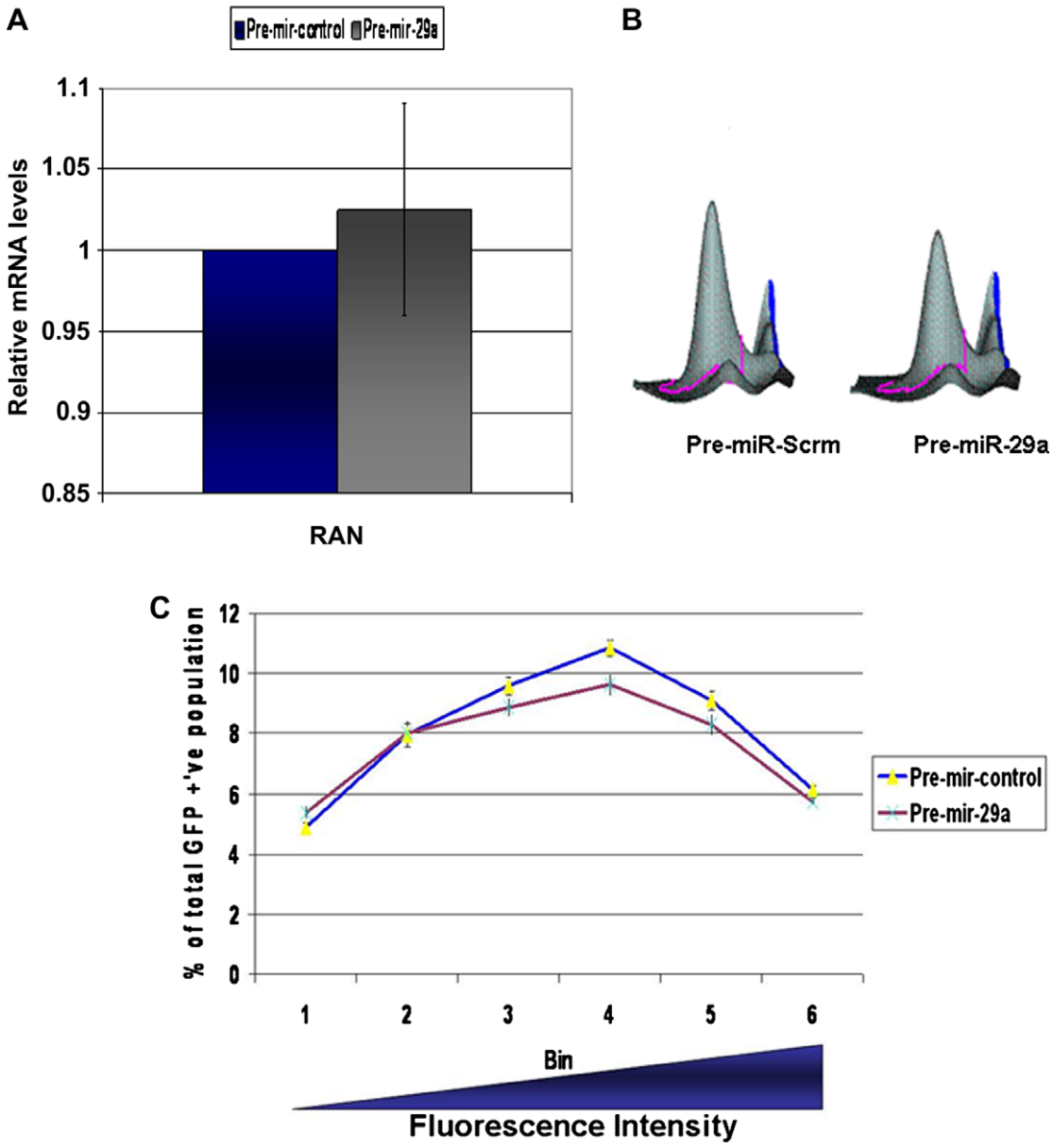

Fig. 6 – (A) Transient transfection of DLKP-A cells with pre-*miR-29a* has no impact on cellular levels of RAN mRNA compared to negative pre-mir control treatment (±SE, $n = 3$). (B) 3-D spot image of same samples analysed by 2D DIGE, the quantity of RAN protein is reduced by >30% ($p < 0.05$). (C) Flow cytometric analysis of GFP fluorescence in mixed, stable, GFP-3′ UTR^{RAN} expressing DLKP cells. Each 'bin' represents the cells with similar fluorescent intensities from low to high.[1–6]

cells. In the case of RAN knockdown, the invasiveness was reduced by 40-80% compared to the invasiveness of the control-transfected cells (Fig. 5a). In addition, cell proliferation was reduced by 30–40% over a 72-h period (Fig. 5b). Knockdown was confirmed at both mRNA and protein levels (Fig. 5c and d). Of the four proteins targeted, only ANXA2 contained a predicted seed region though the RNA hybrid software (http://bibiserv.techfak.uni-bielefeld.de/rnahybrid/) did reveal a weak target site for *miR-29a* in the RAN 3′ UTR (Fig. 5e).

4.5. *Is RAN a direct target of MiR-29a?*

The classical mode of miRNA action typically inhibits target protein translation without concurrent reduction in mRNA abundance. In DLKP-A cells transfected with *miR-29a*, no significant change in RAN transcript levels was detected by qPCR (Fig. 6a) despite a 35% reduction in RAN protein when analysed by 2D DIGE (Fig. 6b). Western blots on the same samples could not reproducibly demonstrate this change in RAN expression (data not shown) as this method lacks the sensitivity of the 2D DIGE approach. Having made the connection between *miR-29a* expression levels, RAN expression and the invasive phenotype, we wished to establish whether *miR-29a* impacted on RAN expression by direct interaction with the mRNA transcript. The RAN 3′ UTR sequence was cloned by PCR from DLKP genomic DNA and placed downstream of a GFP reporter gene. DLKP-A cells, stably expressing this GFP-3′ UTR^{RAN} reporter fusion, were generated and transiently

Table 2 – Panther classification, according to molecular function, of differentially expressed proteins in cells treated with either Pre- or Anti-*miR-29a*. A total of 50 proteins were classified using the DAVID bioinformatics resource (http://david.abcc.ncifcrf.gov/). Count represents number of proteins in each classification group and % represents the percentage of the list of 50 proteins in each group.

Molecular function	Count	%	*p*-Value	GeneBank accession no.
Peroxidase	4	7.27	7.18E–04	NM_006793, NM_005809, NM_002574, NM_004905
Oxidoreductase	7	12.73	0.003381	NM_152740, NM_000454, NM_006793, NM_005809, NM_004544, NM_002574, NM_004905
Transfer/carrier protein	6	10.91	0.00479	NM_015917, NM_001444, NM_018947, NM_002567, NM_001002858, NM_000700
Serine protease inhibitor	11	20.00	0.005989	NM_015917, NM_016045, NM_021130, NM_002305, NM_002796, NM_001008216, NM_024339, NM_002791, NM_002086, NM_002794, NM_002787
Non-receptor serine/threonine protein kinase	15	27.27	0.033791	NM_000485, NM_006817, NM_002796, NM_152265, NM_002075, NM_000975, NM_014362, NM_014412, NM_015917, NM_001540, NM_002415, NM_005809, NM_002629, NM_175054, NM_002794
Other transferase	4	7.27	0.035344	NM_015917, NM_016045, NM_001696, NM_014362,
Annexin	4	7.27	0.039542	NM_198175, NM_001002858, NM_005101, NM_000700
Non-motor actin-binding protein	13	23.64	0.042818	NM_006817, NM_001008216, NM_000975, NM_014362, NM_002791, NM_002086, NM_005507, NM_001444, NM_002305, NM_001540, NM_006012, NM_002629, NM_002787
Protease	5	9.09	0.052485	NM_002796, NM_006012, NM_002791, NM_002794, NM_002787
Chaperone	3	5.45	0.058427	NM_001540, NM_002013, NM_003372
Other isomerase	4	7.27	0.078832	NM_021130, NM_000194, NM_002572, NM_002013
Neuropeptide	4	7.27	0.091305	NM_015917, NM_002567, NM_002075, NM_014362
Other proteases	4	7.27	0.096733	NM_002796, NM_002791, NM_002794, NM_002787

transfected with pre-*miR-29a* or control negative sequence. Flow cytometry analysis revealed that the mean cell fluorescence was not significantly impacted across this mixed population of stable cells in response to pre-*miR-29a* transfection (Fig. 6c).

5. Discussion

Several recent publications have established *miR-29* family members as important molecules in suppressing tumourigenic phenotypes in cell line models. *In vivo*, their expression levels have been shown to positively correlate with favourable outcome in AML patients.[6] Though several important target genes have been identified, typically by homology-based analysis of 3'UTR regions, it is expected that most miRNAs have the potential to influence the expression of many, if not hundreds of target proteins. The list of potential targets identified in this study provides some interesting clues to the different pathways and functions that *miR-29a* might impact on in its role as an 'anti-oncomir'.

Having established that *miR-29a* was down-regulated in invasive lung and pancreatic cell lines, we observed a significant reduction in this phenotype upon re-introduction of exogenous *miR-29a*. Though upregulation of *miR-29a* has been shown to decrease the tumourigenic potential of A549 cells[4] this is the first demonstration of a role in modulating the *in vitro* invasive ability of cancer cells. In addition the effect is not cell- or organ-type specific having demonstrated functional impact in both lung and pancreatic cancer cell lines. Mott and colleagues described a functional role for *miR-29b* in chologiocarcinomas where its enforced expression reduced the cellular levels of Mcl-1 and sensitised cells to TRAIL-mediated cytotoxicity.[3] Furthermore, Pekarsky and colleagues provide evidence that *miR-29b* is involved in suppressing expression of the Tcl1 oncogene which is a causal agent in CLL.[7]

We have shown that invasive DLKP-A cells that stably overexpressed *miR-29a* were also found to have reduced proliferation compared to their control-transfected counterparts and this might be, in part, explained by the ability of *miR-29* family members to down regulate Mcl-1 activity.

The 2D DIGE analysis demonstrated that modifying the cellular concentration of *miR-29a* impacted on the levels of a large number of proteins, with diverse cellular functions. Two lists of differentially expressed proteins were generated using this approach. In an attempt to focus on direct targets of *miR-29a* we limited our analysis to the proteins up-regulated after anti-mir treatment and down-regulated after pre-mir transfection – referred to as the primary list. The assumption here was that the reciprocally effected proteins must be secondary downstream targets of action. Of course further proof would be required to demonstrate that the transcripts coding for the proteins on the primary list are actually directly bound by *miR-29a*.

Using the 'RNA hybrid' software programme to analyse the genes on our primary list, 14 were predicted to contain a 'seed' binding site in their 3′ UTR (at least 6nt match between nt2–8 at 5′ end of the *miR-29a*). This represents less than 20% of the proteins on the list suggesting that either (a) most of the identified proteins are secondary targets of *miR-29a* action or (b) a canonical seed region is not imperative for miRNA-UTR interaction.

Ontological analysis of the differentially expressed proteins revealed a bias towards 4–5 main biological functions including proliferation, apoptosis, motility, differentiation and mutagenesis (Table 1). Likewise, analysis of the main groupings according to molecular function demonstrated an enrichment of peroxidase and oxidoreductase activities (Table 2), again in keeping with previous reports of association of these types of proteins with metastatic tumour formation.[15,16] The predominance of these groupings is in keeping with a role for *miR-29a* in modulating the aggressiveness/invasive potential of cancer cell lines and possibly tumours *in vivo*. Several of the genes identified have well-documented roles in stimulating cellular invasion, such as MIF (macrophage migratory inhibitory factor) which has been implicated in prostate, colon and other cancer types.[17,18] GRB2 (growth factor receptor-bound protein 2) is a crucial adaptor protein that mediates cell signalling from the surface membrane receptors to their downstream targets and indeed is a current target for the development of anticancer therapeutics.[19,20] It was interesting to observe that, despite being identified in the proteomic analysis, subsequent qPCR analyses of both *miR-29a*-transfected and untransfected cells indicated extremely low levels of GRB2 transcript (data not shown).

Several peroxiredoxin family members were identified as being down-regulated in response to *miR-29a* transfection supporting several reports correlating their expression with cancer development and recurrence.[21,22] As antioxidants these proteins might be expected to play a protective role against elimination of cancerous cells *in vivo*.

Enolase (ENO1) is another protein with a recognised role in cellular invasion as a plasminogen-binding receptor.[23] Intriguingly, an alternative splice-variant of this gene, c-myc-promoter binding protein, acts as a transcriptional repressor of c-myc which in turn has been shown recently to repress expression of *miR-29a*.[8] More recently, ENO1 has also been shown to suppress the Notch1 receptor/YY1-dependent activation of *c-myc*.[24] These observations suggest the possibility of a feedback loop where increased *c-myc* expression reduces *miR-29a* levels hence releasing a translational block on ENO1 which in turn antagonises the activation of *c-myc*, thereby releasing *miR-29a* expression and so on.

SFRS1 (splicing factor, arginine/serine-rich 1) was found to be decreased in Herceptin-treated ErbB2-overexpressing cell lines and was also shown to affect cellular motility.[25,26] Our analysis also reveals a predicted *miR-29a* binding site in the 3′ UTR of SFRS1. Galectin-1 (LGALS1) has an established role in the invasive and metastatic potentials of cells *in vitro* and *in vivo*.[27,28] Interestingly there were also examples of genes identified here that have previously been associated with reduction of this phenotype or negatively correlating with poor outcome in clinical studies. Both annexins A1 and A2 are identified as *miR-29a*-regulated genes in this study and both have previously been shown to reduce cell migration *in vitro* and to be lost in some nodal metastases.[29,30] Indeed ANXA2 has a predicted 6nt seed match in its 3′ UTR. The same is true of RKIP (Raf-1 kinase inhibitory protein) which is typically reported to have a metastasis-suppressor role in tumours.[31] However, most of the proteins that have already been linked to cancer or invasion would be expected to be up-regulated based on the reports in the literature in this phenotype – supporting the theory of an anti-invasive role for *miR-29a* in cells.

Rather than focusing solely on the genes that contained predicted *miR-29a* target sites in their 3′ UTRs we chose a small group of targets representing proteins with established roles in the phenotype of interest. Knockdown of the expression levels of these targets individually with siRNA resulted in a phenotypic impact only in the case of RAN (Ran-GTPase). Indeed the degree to which invasion and proliferation were inhibited in the DLKP-A cells was similar to that observed in the *miR-29a* stably transfected cells. RAN is a small 25 kDa protein that acts as a mediator of nucleocytoplasmic transport. In the nucleus it is loaded with GTP by the chromatin-associated RCC1 complex allowing it to interact with certain transport partners to shuttle proteins and small RNAs (including miRNAs) out of the nucleus.[32] It is intriguing to consider the possibility of *miR-29a* self-regulating its cytoplasmic concentration by directly modulating RAN translation. RAN is also involved in nuclear segmentation during mitosis where it directs the assembly of the mitotic spindle. Kurisetty and colleagues have recently demonstrated that RAN overexpression in a non-invasive rat mammary epithelial cell line results in increased anchorage-independent growth, cell attachment, invasion through Matrigel™ *in vitro* and metastasis in rats.[33] Also, Xia and colleagues found that acute silencing of RAN in various tumour cell types causes aberrant mitotic spindle formation, mitochondrial dysfunction and apoptosis.[34] This dependency was not reflected in other normal cell types.

Having established that *miR-29a* influences the cellular concentration of a critical protein that can impact on both invasion and proliferation we wanted to establish whether the RAN transcript was a direct target of *miR-29a* action. The observation that the average fluorescence signal in cells stably expressing a GFP reporter gene fused to the Ran 3′ UTR was not significantly reduced suggests that the impact on endogenous Ran protein expression (35% down-regulated in proteomics analysis) might be secondary to the effect of *miR-29a*.

Irrespective of whether RAN is a direct or indirect target of *miR-29a* activity we provide evidence suggesting that it is via this mechanism, in part at least, that *miR-29a* influences the invasive and proliferative capacity of cancer cells. Indeed, the RAN-dependent status of many tumours[34] raises the possibility of augmenting *miR-29a* expression as a potential therapeutic intervention.

Conflict of interest statement

None declared.

Acknowledgements

This work was supported by the Higher Education Authority of Ireland via its PRTLI III funding scheme and by Science Foundation Ireland.

REFERENCES

1. Ma L, Weinberg RA. Micromanagers of malignancy: role of microRNAs in regulating metastasis. *Trend Genet* 2008;**24**:448–56.
2. Crawford M, Brawner E, Batte K, et al. MicroRNA-126 inhibits invasion in non-small cell lung carcinoma cell lines. *Biochem Biophys Res Commun* 2008;**373**:607–12.
3. Mott JL, Kobayashi S, Bronk SF, Gores GJ. MiR-29 regulates Mcl-1 protein expression and apoptosis. *Oncogene* 2007;**13**: 6133–40.
4. Fabbri M, Garzon R, Cimmino A, et al. MicroRNA-29 family reverts aberrant methylation in lung cancer by targeting DNA methyltransferases 3A and 3B. *Proc Natl Acad Sci USA* 2007;**104**:15805–10.
5. Baek D, Villén J, Shin C, et al. The impact of microRNAs on protein output. *Nature* 2008;**455**:64–71.
6. Garzon R, Garofalo M, Martelli MP, et al. Distinctive microRNA signature of acute myeloid leukemia bearing cytoplasmic mutated nucleophosmin. *Proc Natl Acad Sci USA* 2008;**105**:3945–50.
7. Pekarsky Y, Santanam U, Cimmino A, et al. Tcl1 expression in chronic lymphocytic leukemia is regulated by miR-29 and miR-181. *Cancer Res* 2006;**66**:11590–3.
8. Chang TC, Yu D, Lee YS, et al. Widespread microRNA repression by Myc contributes to tumorigenesis. *Nat Genet* 2008;**40**:43–50.
9. Cleary I, Doherty G, Moran E, Clynes M. The multidrug-resistant human lung tumour cell line, DLKP-A10 expresses novel drug accumulation and sequestration systems. *Biochem Pharmacol* 1997;**53**:1493–502.
10. Pierce A, Barron N, Linehan R, et al. Identification of a novel, functional role for S100A13 in invasive lung cancer cell lines. *Eur J Cancer* 2008;**44**:151.
11. Meleady P, Henry M, Gammell P, et al. Proteomic profiling of CHO cells with enhanced rhBMP-2 productivity following co-expression of PACEsol. *Proteomics* 2008;**8**:2611–24.
12. van Rooij E, Sutherland LB, Thatcher JE, et al. Dysregulation of microRNAs after myocardial infarction reveals a role of miR-29 in cardiac fibrosis. *Proc Natl Acad Sci USA* 2008;**105**:13027–32.
13. Gebeshuber CA, Zatloukal K, Martinez J. MiR-29a suppresses tristetraprolin, which is a regulator of epithelial polarity and metastasis. *EMBO Rep* 2009;**10**:400–5.
14. Park SY, Lee JH, Ha M, Nam JW, Kim VN. MiR-29 miRNAs activate p53 by targeting p85 alpha and CDC42. *Nat Struct Mol Biol* 2009;**16**:23–9.
15. Nishikawa M, Hashida M. Inhibition of tumour metastasis by targeted delivery of antioxidant enzymes. *Expert Opin Drug Deliv* 2006;**3**:355–69.
16. Nishikawa M. Reactive oxygen species in tumor metastasis. *Cancer Lett* 2008;**18**:53–9.
17. Sun B, Nishihira J, Yoshiki T, et al. Macrophage migration inhibitory factor promotes tumor invasion and metastasis via the Rho-dependent pathway. *Clin Cancer Res* 2005;**11**:1050–8.
18. Meyer-Siegler KL, Iczkowski KA, Leng L, Bucala R, Vera PL. Inhibition of macrophage migration inhibitory factor or its receptor (CD74) attenuates growth and invasion of DU-145 prostate cancer cells. *J Immunol* 2006;**177**:8730–9.
19. Giubellino A, Burke Jr TR, Bottaro DP. Grb2 signaling in cell motility and cancer. *Expert Opin Ther Targets* 2008;**12**: 1021–33.
20. Giubellino A, Gao Y, Lee S, et al. Inhibition of tumor metastasis by a growth factor receptor bound protein 2 Src homology 2 domain-binding antagonist. *Cancer Res* 2007;**67**:6012–6.
21. Quan C, Cha EJ, Lee HL, et al. Enhanced expression of peroxiredoxin I and VI correlates with development, recurrence and progression of human bladder cancer. *J Urol* 2006;**175**:1512–6.
22. Kim JH, Bogner PN, Baek SH, et al. Up-regulation of peroxiredoxin 1 in lung cancer and its implication as a prognostic and therapeutic target. *Clin Cancer Res* 2008;**14**:2326–33.
23. Liu KJ, Shih NY. The role of enolase in tissue invasion ad metastasis of pathogens and tumour cells. *J Cancer Mol* 2007;**3**:45–8.
24. Hsu KW, Hsieh RH, Lee YH, et al. The activated Notch1 receptor cooperates with alpha-enolase and MBP-1 in modulating c-myc activity. *Mol Cell Biol* 2008;**28**:4829–42.
25. Mukherji M, Brill LM, Ficarro SB, Hampton GM, Schultz PG. A phosphoproteomic analysis of the ErbB2 receptor tyrosine kinase signaling pathways. *Biochemistry* 2006;**45**: 15529–40.
26. Ghigna C, Giordano S, Shen H, et al. Cell motility is controlled by SF2/ASF through alternative splicing of the Ron protooncogene. *Mol Cell* 2005;**20**:881–90.
27. Jung TY, Jung S, Ryu HH, et al. Role of galectin-1 in migration and invasion of human glioblastoma multiforme cell lines. *J Neurosurg* 2008;**109**:273–84.
28. Rorive S, Belot N, Decaestecker C, et al. Galectin-1 is highly expressed in human gliomas with relevance for modulation of invasion of tumor astrocytes into the brain parenchyma. *Glia* 2001;**33**:241–55.
29. Tatenhorst L, Rescher U, Gerke V, Paulus W. Knockdown of annexin 2 decreases migration of human glioma cells in vitro. *Neuropathol Appl Neurobiol* 2006;**32**:271–7.
30. Yu G, Wang J, Chen Y, et al. Tissue microarray analysis reveals strong clinical evidence for a close association between loss of annexin A1 expression and nodal metastasis in gastric cancer. *Clin Exp Metastasis* 2008;**25**:695–702.
31. Granovsky AE, Rosner MR. Raf kinase inhibitory protein: a signal transduction modulator and metastasis suppressor. *Cell Res* 2008;**18**:452–7.
32. Clarke PR, Zhang C. Spatial and temporal coordination of mitosis by Ran GTPase. *Nat Rev Mol Cell Biol* 2008;**9**:464–77.
33. Kurisetty VV, Johnston PG, Johnston N, et al. RAN GTPase is an effector of the invasive/metastatic phenotype induced by osteopontin. *Oncogene* 2008;**27**:7139–49.
34. Xia F, Lee CW, Altieri DC. Tumor cell dependence on Ran-GTP-directed mitosis. *Cancer Res* 2009;**68**:1826–33.